Journal of Molecular Catalysis A: Chemical 363–364 (2012) 328–334

Contents lists available at SciVerse ScienceDirect

Journal of Molecular Catalysis A: Chemical

journal homepage: www.elsevier.com/locate/molcata

Vanadium-containing nickel phosphate molecular sieves as catalysts for α-pinene oxidation with molecular oxygen: A study of the effect of vanadium content on activity and selectivity

M.N. Timofeeva[a,b,*], Zubair Hasan[c], V.N. Panchenko[a], I.P. Prosvirin[a], Sung Hwa Jhung[c,**]

[a] Boreskov Institute of Catalysis SB RAS, Prospekt Akad. Lavrentieva 5, 630090 Novosibirsk, Russian Federation
[b] Novosibirsk State Technichal University, Prospekt K. Marksa 20, 630092 Novosibirsk, Russian Federation
[c] Department of Chemistry and Green-Nano Materials Research Center, Kyungpook National University, Sankyuck-Dong, Buk-Ku, Daegu 702-701, Republic of Korea

ARTICLE INFO

Article history:
Received 7 May 2012
Received in revised form 30 June 2012
Accepted 8 July 2012
Available online 17 July 2012

Keywords:
Nickel phosphate molecular sieve
VSB-5
Vanadium
Oxygen
α-Pinene
Oxidation

ABSTRACT

Vanadium-containing nickel phosphate molecular sieves (V-VSB-5) were applied as heterogeneous catalysts for the liquid phase oxidation of α-pinene with molecular oxygen at 60 °C. It has been found that the vanadium content in V-VSB-5 materials affects the conversion of α-pinene and product distribution. The conversion of α-pinene increases with increasing of V content. The major products were α-pinene oxide, verbenol and verbenone. Acid–base properties of V-VSB-5 affect the distribution of by-products formed via the isomerization of α-pinene oxide over Lewis acid sites and Brönsted acid sites to campholenic aldehyde and trans-carveol. The increase in V content in V-VSB-5 leads to the increase in isomerization of α-pinene oxide to trans-carveol and decrease in that to campholenic aldehyde.

© 2012 Elsevier B.V. All rights reserved.

1. Introduction

Metal phosphate molecular sieves (MPMS) are widely used in the synthesis of speciality and fine chemicals due to their unique physicochemical properties, such as high stability, microporosity and large surface area [1,2]. Nickel phosphate molecular sieves, such as VSB-1 and VSB-5, have particular interest among various MPMS [3–6]. New discoveries and insights into the physicochemical and catalytic properties of these materials and their derivatives have been reported [7–9]. For example, high activity of VSB-5 was demonstrated in oxidation processes, such as the oxidation of alcohols to corresponding aldehydes or ketones under mild conditions with molecular oxygen [4] and in epoxidation of cyclohexene, cyclooctene [5] and cyclododecene [10] with H_2O_2. The isomorphous substitution of transition metal ions in the VSB framework can strongly change physicochemical properties. Thus, according to FT-IR spectroscopy using $CDCl_3$ as a probe molecule the strength of the strong basic sites (proton affinity, PA) of VSB-5 increases the insertion of iron ions into VSB-5 network from 843 kJ/mol to 925 kJ/mol for 6.5% Fe-VSB-5 [7]. Note that the strength of the strong basic sites for 6.5% Fe-VSB-5 is essentially higher than that of Fe-containing silica materials. Moreover, iron ions into VSB-5 framework can act as active sites for reversible multielectron redox transformations in the course of catalytic reaction that was demonstrated in the phenol hydroxylation and wet phenol oxidation with H_2O_2 [7]. Remarkably, the increase in iron content in Fe-VSB-5 led to the increase in the reaction rates. In contrast to iron ions vanadium ions substitute phosphorus ions in VSB network [11,12]. It can be assumed that insertion of vanadium ions mainly will lead to an increase in the surface acidity that may be also useful for catalysis. Effect of surface acid sites on activity of vanadium-containing materials, such as vanadium-containing mesoporous silica, vanadium-containing zeolites and VAPO/VSAPO, were demonstrated in oxidative dehydrogenation of n-propane to propylene [13–15] and oxidation/ammoxidation of toluene and benzyl alcohol over VAPO [16].

In this paper, we investigated physicochemical and catalytic properties of the vanadium-containing VSB-5 materials (V-VSB-5). Note that properties of V-VSB-5 materials are not investigated until now. The main attention was focused on changes in the nature of surface functional groups after the insertion of V ions in the VSB framework. The catalytic properties of V-VSB-5 were assessed

* Corresponding author at: Boreskov Institute of Catalysis SB RAS, Prospekt Akad. Lavrentieva 5, 630090 Novosibirsk, Russian Federation. Tel.: +7 383 330 7284; fax: +7 383 330 8056.
** Corresponding author. Tel.: +82 53 950 5341; fax: +82 53 950 6330.
E-mail addresses: timofeeva@catalysis.ru (M.N. Timofeeva), sung@knu.ac.kr (S.H. Jhung).

1381-1169/$ – see front matter © 2012 Elsevier B.V. All rights reserved.
http://dx.doi.org/10.1016/j.molcata.2012.07.008

Table 1
Chemical composition of VSB-5 and V-VSB-5 samples.

Sample	Preparation gel (atomic ratio)			V-VSB-5 product					
				Weight content (wt.%)			Atomic ratio		
	x[a]	P/Ni	$\frac{V}{V+Ni+P}$	V	Ni	P	P/Ni	P/V	$\frac{V}{V+Ni+P}$
VSB-5	0	0.63	0	0	48.5	16.8	0.62	0	0
1.1% V-VSB-5	0.042	0.63	2.5	1.1	44.4	14.5	0.59	21.4 (25.6)[b]	1.7 (2.0)[b]
1.7% V-VSB-5	0.068	0.63	4.0	1.7	46.5	16.6	0.64	15.5 (14.5)[b]	2.5 (3.2)[b]

[a] Molar composition of reaction mixture is xVOSO$_4$:0.63H$_3$PO$_4$:1.0NiCl$_2$:3.0NH$_3$:100H$_2$O.
[b] XPS data.

for α-pinene oxidation with molecular oxygen under mild conditions. The oxygenated derivatives of α-pinene, such as verbenol, verbenone and α-pinene epoxide are an important renewable feedstock for flavor and fragrance industries [17]. Thus, verbenone is used for the preparation of taxol, which is introduced as a therapeutic agent [18]. Therefore, the development of catalytic methods for the selective oxidation of α-pinene over heterogeneous catalysts is a challenging goal of fine chemistry. Recently, the oxidation of α-pinene with molecular oxygen was demonstrated in the present of various catalytic systems, such as cobalt-containing systems [19–21], gold catalysts [22], uranyl-containing MCM-41 [23], manganese-containing systems [24–26], Ru- and Pd-containing materials [18,27]. It is well-known that α-pinene oxidation with molecular oxygen proceeds via a free radical chain mechanism with formation of verbenol and verbenone (the allylic oxidation products). The addition of catalysts allows to improve selectivity toward to products of epoxidation, essentially to α-pinene epoxide. Stability of this product depends on the acid properties of catalyst. Thus, rearrangement of α-pinene epoxide into α-campholenic aldehyde over Lewis acid sites of Ti- and Co-containing materials was demonstrated [28,29]. In the presence of Brönsted acids α-pinene epoxide rearrange into trans-carveol [27,28]. Because of this reason, the relationships between the nature of the surface functional groups, the vanadium state and catalytic activity of V-VSB-5 materials were investigated.

2. Experimental

2.1. Synthesis of V-VSB-5 materials

The VSB-5 and V-VSB-5 materials were hydrothermally synthesized with microwave irradiation using $NiCl_2{\cdot}6H_2O$ (Sigma–Aldrich), $VOSO_4{\cdot}xH_2O$ (Sigma–Aldrich, x: 3–5), and ortho-phosphoric acid (H_3PO_4, 85 wt%, OCI chemicals) as Ni, P, and V sources [11]. The designation and chemical composition of the samples are presented in Table 1.

2.2. Instrumental measurements

The porous structure of the materials was determined from the N_2 adsorption isotherms obtained at −196 °C using a Micromeritics ASAP 2400 equipment. The X-ray diffraction patterns were measured on a X-ray diffractometer XRD (ThermoARL) with Cu-K$_\alpha$ (λ = 1.5418 Å) radiation. The morphology of the V-VSB-5 samples was examined using a field emission scanning electron microscope (Hitachi, S-4300). The chemical analyses were done by means of an inductively coupled plasma-atomic emission spectrometry (ICP-AES).

Photoelectron spectra were recorded using SPECS spectrometer with PHOIBOS-150-MCD-9 hemispherical energy analyzer and X-ray monochromator FOCUS-500 (Al K$_\alpha$, irradiation, $h\nu$ = 1486.74 eV, 200 W). The samples were supported onto double-sided conducting copper scotch tape. Binding energy (BE) scale was preliminarily calibrated by the position of the peaks of Au4f$_{7/2}$ (BE = 84.0 eV) and Cu2p$_{3/2}$ (BE = 932.67 eV) core levels. The binding energy of peaks was calibrated by the position of the C1s peak (BE = 284.8 eV) corresponding to the surface hydrocarbon-like deposits (C—C and C—H bonds). The ratio of surface atomic concentrations of the elements was calculated from the integral intensities of photoelectron peaks corrected by corresponding atomic sensitivity factors [30]

DR-UV–vis spectra were obtained using a UV-2501 PC Shimadzu spectrometer with an IRS-250A accessory in the 190–900 nm range with a resolution of 2 nm. These spectra were recorded on $BaSO_4$ which was used as a standard. The sample (particle size 26–50 mesh) was packed in DR-UV–vis cell and treated at necessary conditions.

For IR transmission measurements, the samples were pressed into self-supporting wafers (7–20 mg cm^{-2}) and pre-treated within the IR cell by heating at 250 °C under airflow for 1 h and under vacuum for 0.5 h at 250 °C before adsorption experiments. Then the samples were exposed to saturated pyridine vapors at room temperature for 10 min and under vacuum for 15 min at 150 °C. Then pyridine was desorbed until a pressure of 10^{-2} torr. The strength of Brönsted acid sites of VSB-5 and V-VSB-5 samples was characterized by the proton affinity values (PA) calculated using the equation

$$PA = \frac{\log(3400 - \nu_{NH})}{0.0023} - 51 \quad (1)$$

where PA (kJ mol^{-1}) is the energy of proton elimination from the acid residue, 3400 cm^{-1} is the wavenumber of the band of the undisturbed N—H bond of the pyridinium ion, and ν_{NH} (cm^{-1}) is the wavenumber of the center of gravity of the band of the stretching vibration of the pyridinium ion, which depends on the basicity of the acid residue and determined from the contour of the ν_{NH} band [31].

The amount of Brönsted and Lewis acid sites was estimated from the intensity of the band of the stretching vibration of pyridinium ions with a maximum at 1540 and 1450 cm^{-1} using the equation

$$A = 10^{-3} \cdot A_0 \cdot C_s \cdot \rho, \quad (2)$$

where A is the integral intensity of the band (cm^{-1}); A_0 is the integral intensity of the band at 1 μmol of pyridine adsorbed on 1 g of sample; C_s is the amount of pyridine adsorbed on sample; ρ is the thickness of tablet (mg cm^{-2}) ($A_0^{1545-1548\,cm^{-1}} = 3\,cm^2\,\mu mol^{-1}$ and $A_0^{1450\,cm^{-1}} = 3.26\,cm^2\,\mu mol^{-1}$) [31].

For the analysis of the surface basicity the samples were exposed to saturated $CDCl_3$ vapors for 3 min at room temperature. The spectra were obtained both before and after $CDCl_3$ adsorption, and the difference was calculated. The strength of the basic sites was estimated from the shift of ν_{C-D} using the following equation [7]:

$$\log \nu_{C-D} = 0.0066PA - 4.36, \quad (3)$$

where ν_{C-D} is the shift, in cm^{-1}, of C–D vibration and PA is the proton affinity.

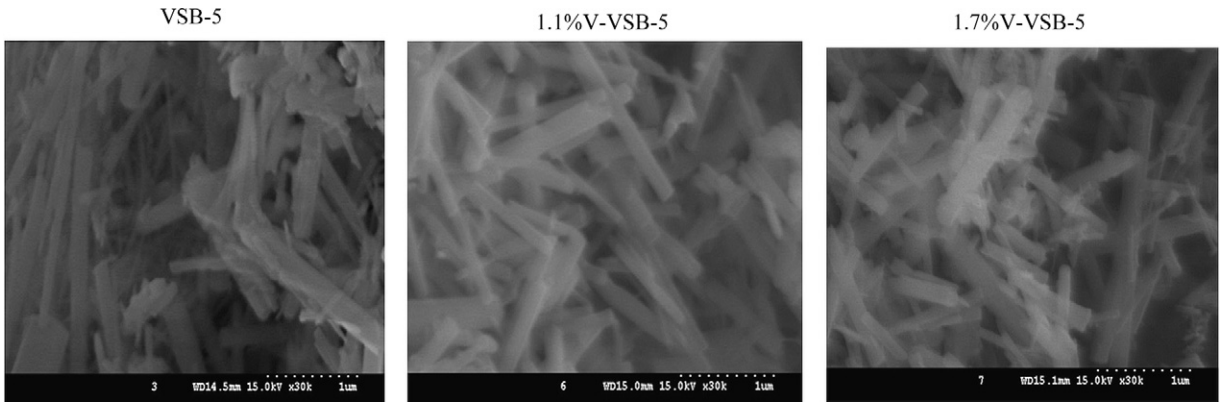

Fig. 1. SEM images of VSB-5 and V-VSB-5 samples.

2.3. Catalytic tests

α-Pinene oxidation was carried out at 60 °C in a glass thermostatted vessel equipped with a stirrer. The reactor was charged with a mixture of 0.05–0.20 mmol α-pinene in 2 ml CH_3CN, 10–20 mg catalyst and then system was saturated by oxygen (V_{gas}/V_{liq} – 6/1 vol vol^{-1}). After running for 5 h under magnetic stirring at 60 °C, the reactor was cooled down to room temperature. The products, after centrifugal separation from the catalyst, were analyzed using a gas chromatograph (Agilent 7820) with a flame ionization detector on capillary column HP-5 and GC-MASS (mass-spectrometer Shimadzu GCMS QP-2010 Ultra).

3. Results

3.1. Physicochemical properties of V-VSB-5

Microporous nickel phosphates V-VSB-5 samples with different vanadium content were synthesized using $VOSO_4$ as a vanadium source according to Ref. [11]. The chemical composition and textural data of V-VSB-5 are shown in Tables 1 and 2, respectively. According to the scanning electron microscopy (SEM) images (Fig. 1) and XRD data (Fig. 2), the crystallinity and morphology of VSB-5 did not change substantially after phosphorus ions substituted by vanadium ions. Note that chemical composition, morphology and XRD spectra of samples are similar to those of V-VSB-5 published in literature [11]. After insertion of vanadium ions into VSB-5 network, XRD reflections in VSB-5 spectrum shift from 5.91°, 9.95° and 11.51° to 5.78°, 9.85° and 11.37° (Fig. 2), respectively. This phenomenon was observed formerly and was explained by the substitution of phosphorus ions to vanadium ions [11].

The oxidation and coordination states of vanadium ions in V-VSB-5 samples were studied by diffuse reflectance UV–visible spectroscopy, and the results are shown in Fig. 3A. The bands at 24,600 and 14,500 cm^{-1} can be assigned to the transitions of octahedral Ni^{2+} ions, $^3A_{2g} \rightarrow {}^3T_{1g}$ (F) and $^3A_{2g} \rightarrow {}^3T_{1g}$ (P), respectively [32]. It is well-known that the structures and oxidation states of vanadium-containing materials have characteristic bands which allow distinguishing V^{5+} from V^{4+}. According to Refs. [33–36] the region 30,000–20,000 cm^{-1} can be assigned to the low-energy ligand-to-metal charge-transfer (LMCT) from O to octahedral V^{5+} ions (V^{5+}, O_h). At the same time the region 35,000–30,000 cm^{-1} ascribes to the low energy LMCT from O to lower coordination tetrahedral V^{5+} ions (V^{5+}, T_d), while the region 35,000–40,000 cm^{-1} assigns to the LMCT from O to V^{4+}. The d–d transitions of VO^{2+} appear at about 13,000 cm^{-1} ($b_2(d_{xy}) \rightarrow (d_{xy},d_{yz})$). As can be seen from DR-UV–vis spectra of V-VSB-5 (Fig. 3A) the insertion of V into VSB-5 network leads to appearance of a broad unresolved band in the region of 46,000–42,000 cm^{-1} which can characterize V^{5+} ions in tetrahedral coordination. Note that in DR-UV–vis spectra of VAPO-11 and VAPO-31 the bands found in this region (42,000 and 45,600 cm^{-1}) were attributed to V^{5+} ions in tetrahedral coordination [37,38]. Moreover a broad unresolved band was also observed in the region of 42,000–25,000 cm^{-1}. We may suggest that in spectra of V-VSB-5 the broad band in the regions of 40,000–27,000 cm^{-1} point to the existence of the four-coordinated V^{4+} (42,000–35,000 cm^{-1}), four- and six-coordinated V^{5+} (35,000–27,000 cm^{-1}) and extra-framework V^{5+} ions in di- or oligomeric V_xO_y structures (31,200–25,000 cm^{-1}). The intensity of this broad band increases with increasing vanadium content. Therefore, DR-UV–vis spectra of V-VSB-5 (Fig. 3A) point to the existence mainly tetrahedral-like vanadium ions.

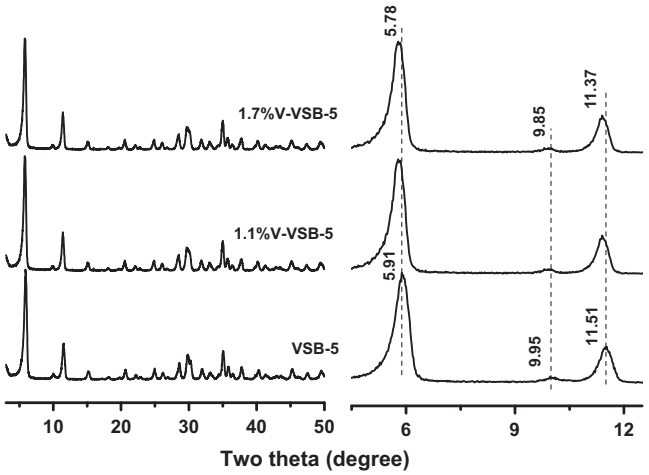

Fig. 2. XRD patterns of VSB-5 and V-VSB-5 samples.

Table 2
Textural data of V-VSB-5 samples.

Sample	S_{BET} (m^2 g^{-1})	S_{ext} (m^2 g^{-1})	V_Σ (cm^3 g^{-1})	V_μ (cm^3 g^{-1})
VSB-5	284	36	0.242	0.128
1.1% V-VSB-5	270	35	0.212	0.131
1.7% V-VSB-5	206	24	0.149	0.093

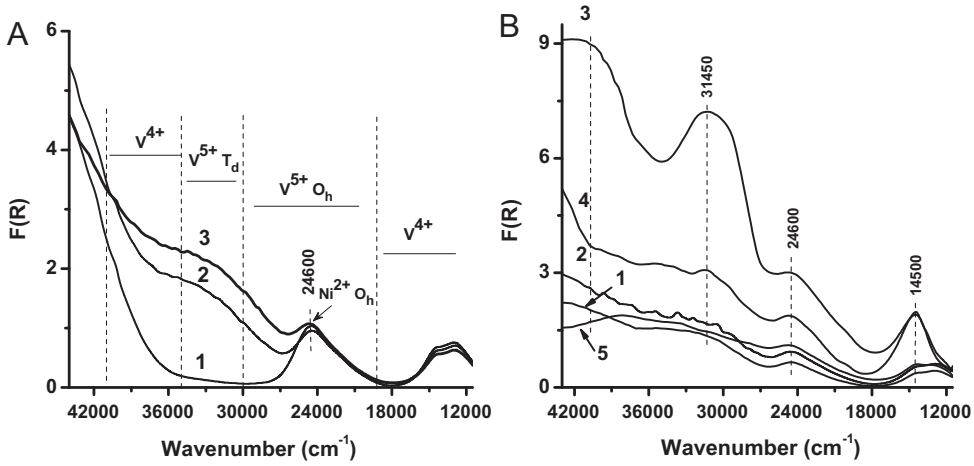

Fig. 3. (A) DR-UV–vis spectra of VSB-5 (1), 1.1% V-VSB-5 (2) and 1.7% V-VSB-5 (3) samples; (B) DR-UV–vis spectra of 1.7% V-VSB-5 (1), α-pinene adsorbed on 1.7% V-VSB-5 in N_2 atmosphere at 25 °C (2), 1.7% V-VSB-5 heated with α-pinene in N_2 atmosphere at 70 °C for 30 min (3) and then in air at 70 °C for 3 h (4) and for 17 h (5).

X-ray photoelectron spectroscopic (XPS) data of VSB-5 and V-VSB-5 samples are shown in Fig. 4 and Table 1. Table 1 shows the result of bulk and surface analyses on the V-VSB-5 samples by XPS measurements. According to these data, the surface P/V, Ni/P and V/(V + Ni + P) atomic ratios are similar to the bulk ratios, indicating that concentrations of Ni, P and V on the surface are close to those in bulk of samples. The XPS spectra of V-VSB-5 samples in $V2p_{3/2}$ and V2p region are shown in Fig. 4. The peak of $V2p_{3/2}$ can be described as the sum of two components centered at 517.1 eV (A) and 516.1 eV (B). The position of component (A) agrees well with the $V2p_{3/2}$ binding energy for V^{5+} oxidation state [39,40], while position of component of (B) can be attributed to V^{4+} oxidation state [39]. These results and DR-UV–vis data confirm our contention that V-VSB-5 samples contain both V^{4+} and V^{5+} states, among them, V^{5+} content is more in 1.7% V-VSB-5 sample.

Based on scientific approach for description of V-sites in VAPO [41] we can assume that at low vanadium content (less than 1 wt% V) in V-VSB-5 V species are monomeric octahedral vanadium (V^{4+}), which partially oxidized to V^{5+} a tetrahedral vanadium species in the course of synthesis of V-VSB-5. Note that V ions can only substitute for P^{5+} ions into VSB network. With higher vanadium content V species might form dimeric and another vanadium (V—O—V) species due to the coupling. Like in mechanism 2 for Si^{4+} substitution in silico-aluminophosphates (SAPOs) these vanadium (V—O—V) species may substitute for Ni—O—P fragments.

3.2. The nature of the surface functional groups of V-VSB-5

It is well-known that catalytic activity and selectivity depend on the nature and strength of active sites in structure of the molecular sieve. Both base and acid sites can contribute to the adjustment of catalytic properties. Because of this reason we have investigated the nature of V-VSB-5 materials by FT-IR spectroscopy using $CDCl_3$ and pyridine as probe molecules.

Basicity of V-VSB-5 materials was studied by FT-IR spectroscopy using $CDCl_3$ as a probe molecule. Previously, this method allows us to reveal and estimate the strength of basic sites in Fe-VSB-5 and VSB-5 materials [7]. It was demonstrated that VSB-5 possesses weak basic sites formed by the Ni ions in the skeleton. The insertion of iron ions into VSB-5 network led to the formation of strong basic sites. At the same time according to our investigation of V-VSB-5 the insertion of vanadium ions into VSB-5 network does not

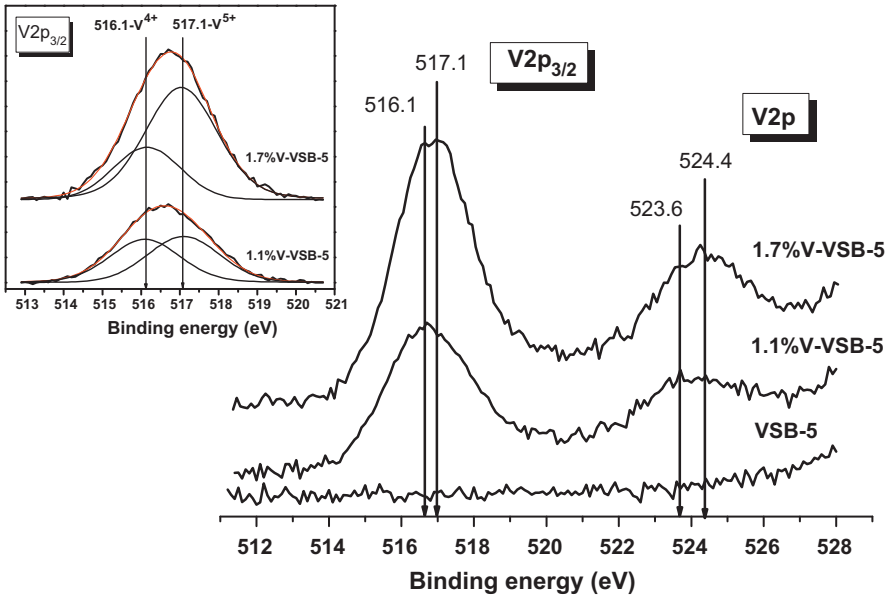

Fig. 4. The $V2p_{3/2}$ and V2p XPS spectra of V-VSB-5 samples.

Table 3
Spectral characteristics (ν_{C-D}) of $CDCl_3$ adsorbed on VSB-5 and V-VSB-5 samples.

Sample	ν_{C-D} (cm^{-1})	$\Delta\nu_{C-D}$ (cm^{-1})	PA ($kJ\,mol^{-1}$)
$CDCl_3$	2268	–	–
VSB-5	2262	6	767
	2252	16	843
1.7% V-VSB-5	2262	6	767
	2252	16	843
6.5% Fe-VSB-5 [7]	2254	14	834
	2212	56	925

change the nature of basic sites. The values for the proton affinity (PA) for VSB-5, Fe-VSB-5 and V–VSB-5 are presented in Table 3. These data show that the insertion of vanadium ions in VSB-5 network is not accompanied by an increase of the strength of the basic sites. The strength of the basic sites of 1.7% V-VSB-5 ($843\,kJ\,mol^{-1}$) is close to that of the strong basic sites of VSB-5 ($843\,kJ\,mol^{-1}$). This result is not surprising, because incorporated vanadium ions possess acidic properties in contrast to iron ions, whose insertion into VSB-5 network leads to an increase in the strength of basicity (Table 3).

The effect of vanadium content in V-VSB-5 on surface acidity was investigated by adsorption of pyridine and the organic indicator of phenolic red. The organic indicator of phenolic red is widely used in acid–base titrations due to the ability to change the color with pH. Phenolic red has red and yellow colors in alkaline solutions (pH > 8.4) and weak acid solutions (pH < 6.8), respectively. According to experimental evidence the color of phenolic red adsorbed onto V-VSB-5 samples from aqueous solution depends on vanadium content (Fig. 5). The colors of indicator adsorbed onto V-VSB-5 changes from red to yellow with increase in vanadium content. Based on this change in colors we can assume that the strength of acid sites decreases in the order:

1.7% V-VSB-5 > 1.1% V-VSB-5 > VSB-5.

This result is an agreement with the result obtained by FT-IR spectroscopy using pyridine as probe molecules (Table 4). The values for the proton affinity (PA) allude to the fact that the insertion of V ions into VSB network leads to the increase in surface acidity. The

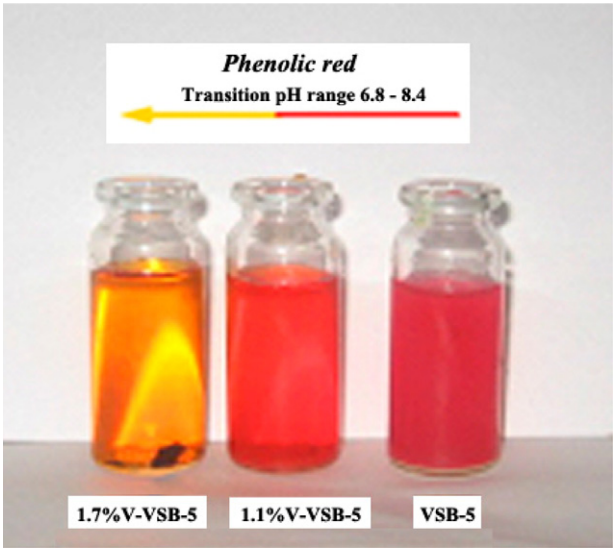

Fig. 5. The color of phenolic red adsorbed onto VSB-5 and V-VSB-5 materials. (For interpretation of the references to color in this figure legend, the reader is referred to the web version of the article.)

Table 4
Brönsted and Lewis acidity of V-VSB-5 materials determined by FTIR spectroscopy using pyridine as probe molecules.

Sample	Brönsted acid sites[a]		N_{LAS}/N_{BAS} ($mol\,mol^{-1}$)
	N_{BAS} ($\mu mol\,g^{-1}$)	PA ($kJ\,mol^{-1}$)	
VSB-5	1.0	1213	1.8
1.1% V-VSB-5	2.7	1196	1.3
1.7% V-VSB-5	4.9	1158	0.9

[a] Amounts of Brönsted and Lewis sites were estimated based on a.b. at 1545 and 1450 cm^{-1}, respectively.

strength of Brönsted acid sites (PA) decreases in the order (Table 4):

1.7% V-VSB-5 > 1.1% V-VSB-5 > VSB-5

In this order an amount of Brönsted acid sites decreases, while the amount of Lewis acid sites increases.

3.3. Catalytic properties of V-VSB-5

The V-VSB-5 materials were tested in oxidation of α-pinene (1) with molecular oxygen at atmospheric pressure in order to understand relationships between chemical composition, physicochemical properties and catalytic performance. As shown in Table 5, the main reaction products are products of epoxidation and allylic oxidation, such as α-pinene epoxide (2), α-campholene aldehyde (3), trans-carveol (4), verbenol (5), verbenone (6) and others (Scheme 1). The molar ratio of allylic oxidation/epoxidation products is about 2/1 that can be account for the domination of the radical-mediated reaction over direct epoxidation due to the different reactivity of the allylic hydrogen toward the abstraction. Selectivities for corresponding products obtained with V-VSB-5 catalysts are comparable with those reported for Co—SiO_2 systems [29] and Pd/C [27]. It is well-known that in autoxidation of alkenes a free radical chain mechanism involves the formation of allylic hydroperoxides, which facilitate the initiation of the free radical [42]. Moreover, Centi and Trifiro [14] suggested that radicals can form due to the oxygen interaction with Brönsted acid sites. At the same time the role of catalyst is generally related to the decomposition of allylic hydroperoxide intermediates.

The obtained results indicate conclusively that conversion of α-pinene and distribution of products depend on the vanadium content in V-VSB-5 materials (Table 5). The increase in vanadium content leads to an increase in the conversion of α-pinene (1). The vanadium content in V-VSB-5 also affects the isomerization of α-pinene oxide (2) to α-campholenic aldehyde (3) and trans-carveol (4) (Scheme 1). The more vanadium content, the more amount of α-pinene oxide transforms to (3) and (4). It is well-known that in the isomerization of α-pinene oxide the distribution of products largely depends on the nature of surface sites [43,44]. It is well-known [28] that the isomerization of α-pinene oxide over Lewis acid sites leads to the formation of campholenic aldehyde (3), while Brönsted acid sites will result in the formation of trans-carveol (4). Data reported in the present work have confirmed this assertion. The increase in the strength of Brönsted sites and molar ratio of Brönsted/Lewis acid sites (Table 4) favors the increase in isomerization rate of α-pinene oxide to trans-carveol and decrease in that to campholenic aldehyde (Table 5).

We have studied catalytic properties and reaction mechanism in the presence of 1.7% V-VSB-5. It was found that the selectivity of allylic oxidation products strongly depended on the consumption of α-pinene in the course of reaction (Fig. 6A). The maximal total selectivity toward ∑(verbenol + verbenone) reached value of 52%

Table 5
α-Pinene oxidation with molecular oxygen over V-VSB-5 materials catalysts.[a]

Sample	Conversion of (1) (%)	Selectivity (mol.%)					Other
		Epoxidation			Allylic products		
		(2)	(3)	(4)	(5)	(6)	
VSB-5	3	25	8	5	32	16	14
1.1% V-VSB-5	12	21	8	9	32	13	17
1.7% V-VSB-5	18	16	6	13	31	17	17
	12[b]	21	9	11	28	21	10
Co—SiO_2/900 °C[c] [21]	40	n.d.	5	–	34	26	9

[a] 0.1 mmol α-pinene (1), 1 atm O_2, 20 mg catalyst in 2 ml CH_3CN, 60 °C, 5 h.
[b] 15 mg 1.7% V-VSB-5 in reaction mixture.
[c] 5 wt.% Co—SiO_2, 1 atm O_2, 60 °C, 24 h.

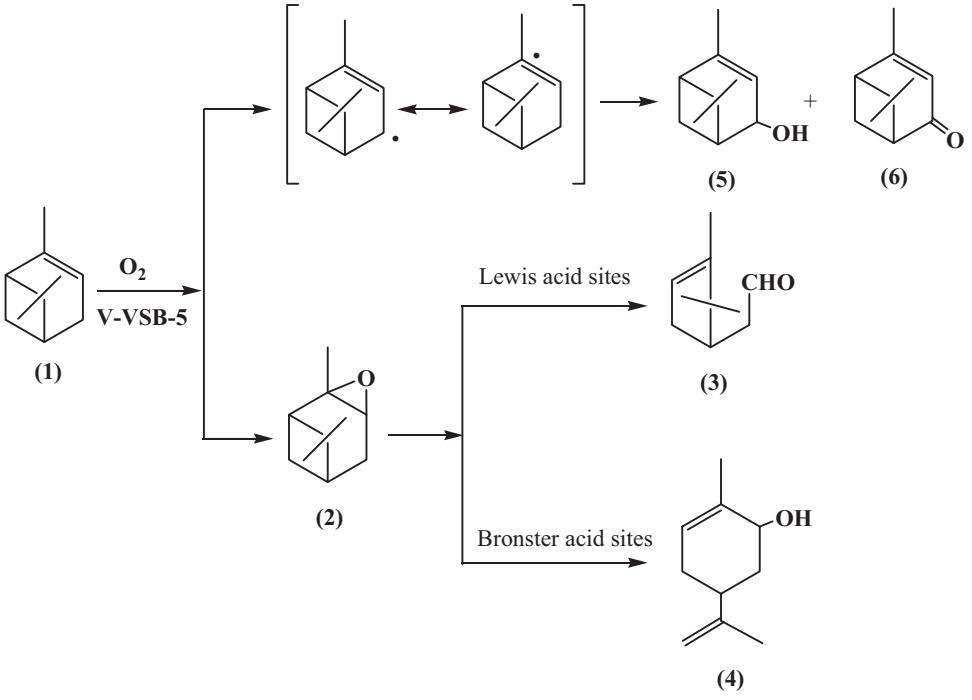

Scheme 1. Reaction pathway of α-pinene oxidation.

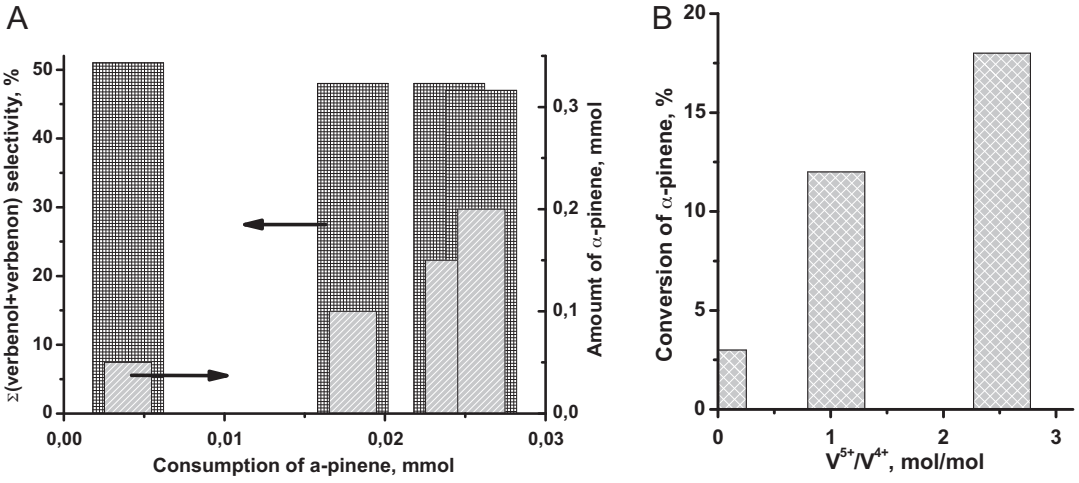

Fig. 6. (A) Correlations between (a) consumption of α-pinene and ∑(verbenol + verbenone) selectivity and (b) consumption of α-pinene and amount of α-pinene in reaction mixture (*Reaction conditions*: 20 mg of 1.7% V-VSB-5 in 2 ml CH_3CN, 60 °C, 5 h); (B) correlation between conversion of α-pinene and V^{5+}/V^{4+} atomic ratio determined by XPS analysis.

at 18% conversion of α-pinene for 5 h. The conversion of α-pinene reduces with decrease in catalyst amount (Table 5).

The catalytic behavior of V-VSB-5 may be related to the presence of tetrahedral V^{5+} species and their one-electron transfer processes, i.e. V^{5+}/V^{4+} valence changes. To obtain information on the oxidation state of vanadium in situ UV–vis spectra of 1.7% V-VSB-5 in the presence of α-pinene were obtained (Fig. 3B). As can be seen from Fig. 3B (curves 1 and 2) spectrum of α-pinene adsorbed on 1.7% V-VSB-5 in N_2 atmosphere at 25 °C is similar to the spectrum of 1.7% V-VSB-5. After heating at 70 °C for 30 min and then adsorption of α-pinene on 1.7% V-VSB-5 in N_2 atmosphere, two strong bands at 31,450 and ~40,000 cm^{-1} are observed in spectrum (Fig. 3B, curve 3), which can be evidently attributed to the LMCT of T_d-coordinated V^{5+} and V^{4+} ions [45]. The intensities of these bands decrease after heating in air at 70 °C (Fig. 3B, curve 4). Note that intensity of band at ~40,000 cm^{-1} changes largely in comparison with that of band at 31,450 cm^{-1}. The obtained results can indicate that vanadium ions are active sites for adsorption of α-pinene molecules and following its catalytic oxidation. These data are in agreement with a correlation between conversion of α-pinene and V^{5+}/V^{4+} molar ratio (Fig. 6B). Of note that similar correlation between V^{5+}/V^{4+} molar ratio and catalytic activity, i.e. the importance of V^{5+} centers, was demonstrated in the selective oxidation of butane to maleic anhydride over vanadium phosphorus catalysts [46,47].

4. Conclusion

In this study physicochemical properties of vanadium-containing nickel phosphate molecular sieves (V-VSB-5) were investigated by XRD, SEM, XPS, N_2-adsorption/desorption analysis DR-UV–vis and FT-IR spectroscopy. According to XPS and DR-UV–vis spectroscopy both V^{4+} and V^{5+} states are observed in V-VSB-5 samples. The increase in vanadium content leads to the increase V^{5+}/V^{4+} molar ratio. It was shown by FT-IR spectroscopy using $CDCl_3$ as a probe molecule that the strength of basic sites for V-VSB-5 (843 kJ mol^{-1}) is close to that for VSB-5 (843 kJ mol^{-1}). The Brönsted acidity was investigated by adsorption of two indicators, such as pyridine and phenolic red. It was found that the strength of Brönsted acid sites increased with increasing of vanadium content in V-VSB. The increase in vanadium content leads to increase in molar ratio of Brönsted/Lewis acid sites.

The catalytic activity of V-VSB-5 was tested for the oxidation of α-pinene with molecular oxygen. The main reaction products are α-pinene epoxide, α-campholene aldehyde, trans-carveol, verbenol and verbenone. It was shown that conversion of α-pinene and distribution of products depends on the vanadium content in V-VSB-5 materials. As the vanadium content in VSB-5 network increased, the conversion of α-pinene increased. Acid–base properties of V-VSB-5 affect the distribution of by-products formed via the isomerization of α-pinene oxide over Lewis acid sites and Brönsted acid sites to campholenic aldehyde and trans-carveol, respectively. The increase in vanadium content in V-VSB-5 leads to the increase in isomerization of α-pinene oxide to trans-carveol and decrease in that to campholenic aldehyde. From DR-UV–vis studies we conclude that the active center for α-pinene constitute a V^{5+} ions that is in agreement with a correlation between conversion of α-pinene and V^{5+}/V^{4+} molar ratio.

Acknowledgements

This work was partly supported by Kyungpook National University Research Fund, 2011. We also thank Dr. N.V. Maksimchuk for productive and beneficial discussion of our results. The authors would like to thank Dr. S.A. Prihod'ko for GC-MASS measurements and discussion.

References

[1] H.O. Pastore, S. Coluccia, L. Marchese, Annu. Rev. Mater. Res. 35 (2005) 351.
[2] M. Hartmann, L. Kevan, Chem. Rev. 99 (1999) 635.
[3] J.-S. Chang, S.-E. Park, Q. Gao, G. Ferey, A.K. Cheetham, Chem. Mater. 9 (2001) 859.
[4] C. Li, H. Kawada, X. Sun, H. Xu, Y. Yoneyama, N. Tsubaki, ChemCatChem. 3 (2011) 684.
[5] S.H. Jhung, J.-H. Lee, A.K. Cheetham, G. Ferey, J.-S. Chang, J. Catal. 239 (2006) 97.
[6] N. Guillou, Q. Gao, M. Nogues, R. Morris, M. Hervieu, G. Ferey, A.K. Cheetham, C. R. Acad. Sci. Ser. IIc 2 (1999) 387.
[7] M.N. Timofeeva, Z. Hasan, A. Yu Orlov, V.N. Panchenko, Yu A. Chesalov, I.E. Soshnikov, S.H. Jhung, Appl. Catal. B: Environ. 107 (2011) 197.
[8] S.-J. Liu, H.-Y. Cheng, F.-Y. Zhao, J.-Y. Gong, S.-H. Yu, Chem. Eur. J. 14 (2008) 4074.
[9] D. Gao, Q. Gao, Catal. Commun. 8 (2007) 681–685.
[10] J. Yu, A. Wang, J. Tan, X. Li, J.A. van Bokhoven, Y. Hu, J. Mater. Chem. 18 (2008) 3601.
[11] S.H. Jhung, J.-S. Chang, Y.K. Hwang, J.-M. Greneche, G. Ferey, A.K. Cheetham, J. Phys. Chem. B 109 (2005) 845.
[12] S.H. Jhung, J.-S. Chang, J.W. Yoon, J.-M. Greneche, G. Ferey, A.K. Cheetham, Chem. Mater. 16 (2004) 5552.
[13] G. Centi, S. Perathoner, F. Trifiro, A. Aboukais, C.F. Aissi, M. Guelton, J. Phys. Chem. 96 (1992) 2617.
[14] G. Centi, F. Trifiro, Appl. Catal. A: Gen. 143 (1996) 3.
[15] T. Blasco, J.M. Lopez Nieto, A. Dejoz, M.I. Vazquez, J. Catal. 157 (1995) 271.
[16] S.J. Kulkarni, R. Rao, M. Subrahmanyam, A.V.R. Rao, A. Sarkany, L. Guczi, Appl. Catal. A: Gen. 139 (1996) 59.
[17] W.F. Erman, Chemistry of the Monoterpenes: An Encyclopedic Handbook, Dekker, New York, 1985.
[18] P.A. Wende, T.P. Muciaro, J. Am. Chem. Soc. 114 (1992) 5878.
[19] T. Joseph, D.P. Sawant, C.S. Gopinath, S.B. Halligudi, J. Mol. Catal. A: Chem. 184 (2002) 289.
[20] E. Blaz, J. Pielichowski, Molecules 11 (2006) 115.
[21] M.V. Patil, M.K. Yadav, R.V. Jasra, J. Mol. Catal. A 277 (2007) 72.
[22] C.D. Pina, E.F. Falletta, M. Rossi, Chem. Soc. Rev. 41 (2012) 350.
[23] P. Selvam, V.M. Ravat, V. Krishna, J. Phys. Chem. C 115 (2011) 1922.
[24] R. Raja, G. Sankar, J.M. Thomas, Chem. Commun. (1999) 829.
[25] W.J. Yang, C.C. Gui, Z.Y. Li, N.Y. Tao, J. Porphyr. Phthalocyan. 13 (2009) 973.
[26] S. Bhattachacharjee, T.J. Dines, J.A. Anderson, J. Catal. 225 (2004) 398.
[27] J.E. Ancel, N.V. Maksimchuk, I.L. Simakova, V.A. Semikolenov, Appl. Catal. A: Gen. 272 (2004) 109.
[28] Y.-W. Suh, N.-K. Kim, W.-S. Ahn, H.-K. Rhee, J. Mol. Catal. A: Chem. 174 (2001) 249.
[29] P.A. Robles-Dutenhefner, M.J. Silva, L.S. Sales, E.M.B. Sousa, E.V. Gusevskaya, J. Mol. Catal. A: Chem. 217 (2004) 139.
[30] J.H. Scofield, J. Electron Spectrosc. Relat. Phenom. 8 (1976) 129.
[31] A.A. Davydov, Molecular Spectroscopy of Oxide Catalyst Surfaces, John Wiley, England, 2003, p. 1.
[32] F.A. Cotton, G. Wilkison, Advanced Inorganic Chemistry, Wiley, New York, 1980, p. 786.
[33] X. Gao, M.A. Banares, I.E. Wachs, J. Catal. 188 (1999) 325.
[34] A. Corma, J.M. Lopez Nieto, N. Paredes, Appl. Catal. A: Gen. 104 (1993) 161.
[35] T. Sen, V. Ramaswamy, S. Ganapathy, P.R. Rajamohanan, S. Sivasanker, J. Phys. Chem. 100 (1996) 3809.
[36] A. Albuquerque, H.O. Pastore, L. Marchese, Stud. Surf. Sci. Catal. 158 (2005) 901.
[37] M. Vishnuvarthan, A.J. Paterson, R. Raja, A. Piovano, F. Bonino, E. Gianotti, G. Berlier, Micropor. Mesopor. Mater. 138 (2011) 167.
[38] M.H. Zahedi-Niaki, S.M.J. Zaidi, S. Kaliaguine, Appl. Catal. A: Gen. 196 (2000) 9.
[39] M. Demeter a, M. Neumann, W. Reichelt, Surf. Sci. 454–456 (2000) 41.
[40] G.A. Sawatzky, D. Post, Phys. Rev. B 20 (1979) 1546.
[41] M.J. Haanepen, J.H.C. van Hooff, Appl. Catal. A: Gen. 152 (1997) 183.
[42] R.A. Sheldon, J.K. Kochi, Metal-Catalyzed Oxidations of Organic Compounds, Academic Press, London, 1981.
[43] G. Neri, G. Rizzo, C. Crisafulli, L. De Luca, A. Donato, M.G. Musolino, R. Pietropaolo, Appl. Catal. A: Gen. 295 (2005) 116.
[44] W.F. Holderich, J. Roseler, G. Heitmann, A.T. Liebens, Catal. Today 37 (1997) 353.
[45] R. Bulanek, L. Capek, M. Setnicka, P. Cicmanec, J. Phys. Chem. C 115 (2011) 12430.
[46] G.J. Hutchings, C.J. Kiely, M.T. Sananes-Schulz, A. Burrows, J.C. Volta, Catal. Today 40 (1998) 273.
[47] M. Abon, J.C. Volta, Appl. Catal. A: Gen. 157 (1997) 173.